



HAL
open science

Chemical nitrogen fractionation in dense molecular clouds

Jean-Christophe Loison, Valentine Wakelam, Kevin Hickson, P. Gratier

► **To cite this version:**

Jean-Christophe Loison, Valentine Wakelam, Kevin Hickson, P. Gratier. Chemical nitrogen fractionation in dense molecular clouds. *Monthly Notices of the Royal Astronomical Society*, 2019, 484 (2), pp.2747-2756. 10.1093/mnras/sty3293 . hal-01982093

HAL Id: hal-01982093

<https://hal.science/hal-01982093>

Submitted on 30 May 2024

HAL is a multi-disciplinary open access archive for the deposit and dissemination of scientific research documents, whether they are published or not. The documents may come from teaching and research institutions in France or abroad, or from public or private research centers.

L'archive ouverte pluridisciplinaire **HAL**, est destinée au dépôt et à la diffusion de documents scientifiques de niveau recherche, publiés ou non, émanant des établissements d'enseignement et de recherche français ou étrangers, des laboratoires publics ou privés.

Chemical nitrogen fractionation in dense molecular clouds

Jean-Christophe Loison¹,^{1★} Valentine Wakelam²,² Pierre Gratier² and Kevin M. Hickson¹

¹*Institut des Sciences Moléculaires (ISM), CNRS, Univ. Bordeaux, 351 cours de la Libération, F-33400 Talence, France*

²*Laboratoire d'astrophysique de Bordeaux, Univ. Bordeaux, CNRS, B18N, allée Geoffroy Saint-Hilaire, F-33615 Pessac, France*

Accepted 2018 November 26. Received 2018 November 26; in original form 2018 July 4

ABSTRACT

Nitrogen-bearing molecules display variable isotopic fractionation levels in different astronomical environments such as in the interstellar medium or in the Solar system. Models of interstellar chemistry are unable to induce nitrogen fraction in cold molecular clouds as exchange reactions for ^{15}N are mostly inefficient. Here, we developed a new gas–grain model for nitrogen fractionation including a thorough search for new nitrogen fractionation reactions and a realistic description of atom depletion on to interstellar dust particles. We show that, while dense molecular cloud gas-phase chemistry alone leads to very low fractionation, ^{14}N atoms are preferentially depleted from the gas phase due to a mass-dependent grain surface sticking rate for atomic nitrogen. However, assuming an elementary $^{14}\text{N}/^{15}\text{N}$ ratio of 441 (equal to the solar wind value), our model leads to only low ^{15}N enrichment for all N-containing species synthesized in the gas phase with predicted $^{14}\text{N}/^{15}\text{N}$ ratios in the range 360–400. Higher enrichment levels can neither be explained by this mechanism, nor through chemistry, with two possible explanations: (i) The elementary $^{14}\text{N}/^{15}\text{N}$ ratio in the local ISM is smaller, as suggested by the recent work of Romano et al., with a hypothetical $^{15}\text{NNH}^+$ and $^{15}\text{NNH}^+$ depletion due to variation of the electronic recombination rate constant variation with the isotopes and (ii) N_2 photodissociation leads to variable nitrogen fractionation in diffuse molecular clouds where photons play an important role, which is conserved during dense molecular cloud formation as suggested by the work of Furuya & Aikawa.

Key words: astrochemistry – ISM: abundances – ISM: clouds.

1 INTRODUCTION

Planetary systems, such as our own Solar system arise from the collapse of a dense molecular cloud (Füri & Marty 2015). Consequently, remnants of earlier evolutionary stages might be expected to be preserved in the composition of Solar system objects. Isotopic abundances are a sensitive probe of the processes leading to the formation of planetary systems as hydrogen, carbon, nitrogen, and oxygen often present large differences in their fractionation ratios between the various steps. Among them, nitrogen fractionation is a key issue. The $\text{N}/^{15}\text{N}$ ratio in the Solar system is equal to 441 ± 2.5 for the main reservoir of N (the Sun's photosphere; Marty et al. 2010), a value that is seemingly incompatible with the elemental ratio in the local interstellar medium (ISM) estimated to be 290 ± 40 (Adande & Ziurys 2012) from interpolation of the galactic gradient using $\text{CN}/\text{C}^{15}\text{N}$ and $\text{HNC}/\text{H}^{15}\text{NC}$ measurements across the Galaxy. This low elemental $\text{N}/^{15}\text{N}$ ratio also seems to agree with the observed $\text{CN}/\text{C}^{15}\text{N}$ and $\text{HCN}/\text{HC}^{15}\text{N}$ ratios in

diffuse molecular clouds (Lucas & Liszt 1998; Ritchey, Federman & Lambert 2011). Such a low elemental ratio may be due to galactic chemical evolution (Romano et al. 2017). Nevertheless, Colzi et al. (2018) found recently a $\text{N}/^{15}\text{N}$ ratio in HCN and HNC across the galaxy much closer to 400, which challenges the Adande & Ziurys (2012) result. Moreover, the measurements may be affected by efficient nitrogen fractionation processes in diffuse or/and dense molecular clouds. To test for possible chemical ^{15}N fractionation in dense molecular clouds, Terzieva & Herbst (2000) developed a chemical model introducing various ^{15}N exchange reactions. Their model resulted in low ^{15}N enrichment, although further studies using their chemical network derived more notable fractionations (Rodgers & Charnley 2008a; Rodgers & Charnley 2008b; Wirstrom et al. 2012). Subsequent work by Roueff, Loison & Hickson (2015), however, clearly demonstrated that the efficient fractionation reactions proposed by Terzieva & Herbst (2000) are characterized by activation barriers and are therefore inefficient at low temperature. Furthermore, recent simulations by Wirstrom & Charnley (2018) showed that the additional fractionation reactions proposed by Roueff et al. (2015) suppressed ^{15}N enrichment in molecules containing the nitrile functional group. To date, no

* Email: jean-christophe.loison@u-bordeaux.fr

astrochemical model based on gas-phase chemistry alone has been able to induce nitrogen fractionation levels greater than a few percent. Although the Wiström & Charnley (2018) model included simplified grain processes such as the depletion of gas-phase species on to grains; grain surface chemistry and grain desorption (with the exception of H₂ desorption) were not included. In addition, N and N₂ depletion was switched off, so any processes induced by nitrogen sticking on grains or by surface chemistry could not be reproduced.

In the absence of alternative viable fractionation reactions, an alternative pathway to consider is N₂ photodissociation as shown by Heays et al. (2014), where N-fractionation arises from the more efficient photodissociation of ¹⁵NN compared with N₂ due to the self-shielding of N₂ at high abundances. In dense molecular clouds, however, photons are almost entirely generated by emission from electronically excited H₂, with fluxes that are too low for this type of process to be efficient. However, Furuya & Aikawa (2018) have developed a model to simulate molecular cloud formation starting from a diffuse H I cloud. In the first part of cloud evolution, UV radiation is high enough to ensure photodissociation. A key point in their model is the quick transformation of N atoms into N₂ and s-NH₃ (s- meaning species on grains) for low visual extinction levels (A_v below 2). Then, photodissociation of N₂ is important, and self-shielding of N₂ leads to preferential N¹⁵N depletion and ¹⁵N enrichment in the gas phase. The N¹⁵N depletion is partly conserved in the dense cloud with large A_v, but their model cannot reproduce the various observations. Indeed, the calculated N₂H⁺/¹⁵NNH⁺ and N₂H⁺/N¹⁵NH⁺ ratios are around 410, far smaller than the high N₂H⁺ depletion levels observed in L1544 and L429 (Redaelli et al. 2018). In their model, nitrogen atoms are rapidly removed from the gas phase and transformed into s-NH₃ (on grains), which is mostly retained on the surface. Then, the gas-phase nitrogen chemistry in dense molecular clouds is initiated by dissociation of N₂ through cosmic rays or by reaction with He⁺. The Furuya & Aikawa (2018) model is indeed very interesting but involves significant approximations due to the importance of grain chemistry in their model, which is not well characterized at all. A better knowledge of grain chemistry, particularly for A_v below 2 where photons can not only photodesorb species but also induce chemical desorption through photodissociation and recombination, is clearly needed.

A critical point for the comparison between observed fractionation levels and astrochemical models are the observational uncertainties. Indeed, for some molecules, the main isotopologue transitions are optically thick, leading to a potential underestimation of abundances, or conversely, uncertainties can be large due to the very weak intensities of the minor isotopologue lines. For HCN, HNC, and CN, the extent of nitrogen fractionation is deduced almost always by the so-called double isotopes ratio method deducing the ¹⁴N/¹⁵N ratio from H¹³CN/H¹⁵CN, HN¹³C/H¹⁵NC, and ¹³CN/C¹⁵N ratios using a ¹²C/¹³C ratio equal to 68 (Milam et al. 2005; Adande & Ziurys 2012). However, Roueff et al. (2015) showed that carbon chemistry leads to variable and time-dependent ¹³C fractionation levels in dense molecular clouds, so that ¹⁵N enrichment levels obtained using the double isotopes ratio method are unreliable. If we ignore the double isotope determinations and most of the cases where the main isotopologue emission lines are highly saturated (requiring complex analyses leading to very high uncertainties (Gonzalez-Alfonso & Cernicharo 1993; Daniel et al. 2013), the range of observed N¹⁵N ratios in dense molecular clouds is much less variable (around 250–350 taking into account the uncertainties, see Table 1), apart from the notable exceptions of N₂H⁺ in L1544 and HCN and HNC in B1. The results of (Daniel et al. 2013) for

B1 are doubtful as noted by the authors themselves. Indeed, even if they accounted for the opacity of the lines in a similar manner to Magalhães et al. (2018), the lines of the main isotopologues were highly saturated. It should be noted that we do not present the results for NH₂D/¹⁵NH₂D observations (see for example Gerin et al. 2009) as we do not consider deuterium chemistry in this work. Indeed, ¹⁵NH₂D formation reaction rate constants are not identical to those of NH₂D (Roueff et al. 2015).

To test the influence of the updated network in the gas phase and the surface chemistry on nitrogen fractionation, we have developed a new gas–grain model including relevant chemical and physical processes. The chemical model including the various updates is presented in Section 2, and the comparison with observations and previous models is described in Section 3. Our conclusions are presented in Section 4.

2 THE CHEMICAL MODEL

To compute the abundances, we use a new chemical network based on the chemical model Nautilus in its 3-phase version (Ruaud, Wakelam & Hersant 2016) using kida.uva.2014 (Wakelam et al. 2015) with updates from Loison et al. (2016), Loison et al. (2017), and Vidal et al. (2017) for the chemistry. In the 3-phase model, we make a distinction between the first two monolayers of molecules on top of the grains (considered as the surface) and the rest of the layers below (considered as the bulk), the gas being the third phase. In this model, only molecules at the surface can desorb (direct thermal desorption, chemical desorption, cosmic ray-induced desorption, and photodesorption). Species can, however, diffuse in both the surface and the bulk but with a much smaller efficiency in the bulk. To compute the surface probability of reaction for reactions with activation barriers, we consider the competition between reaction, diffusion, and evaporation. Diffusion by tunnelling is considered only for reactions involving hydrogen atoms. Cosmic ray-induced photodissociations can occur through both grain phases. All details of the equations and model parameters not specifically discussed in this article are the same as in Ruaud et al. (2016).

The new network is limited to a carbon skeleton up to C₃H_xN_y (x = 0–2, y = 0–1) and C₃H_xN_y⁺ (x = 0–2, y = 0–1), to reduce the number of reactions when considering all ¹⁵N species. It includes 4641 reactions in the gas phase and 5154 reactions on grains including the reactions between the surface and the bulk as well as photodissociation. The new network reproduces the abundances of the complete network for the main species studied here. We have also introduced ¹⁵N exchange reactions using an updated version of the network presented in Roueff et al. (2015) and some new exchange reactions using recent published works.

The surface network is similar to the one in Ruaud et al. (2015) with some updates from Wakelam et al. (2017). Following Hincelin, Chang & Herbst (2015), the encounter–desorption mechanism is included in the code. This mechanism accounts for the fact that the H₂ binding energy on itself is much smaller than on water ices and prevents the formation of several H₂ monolayers on grain surfaces.

The accretion rate for a species *i* is described by the following classical expression

$$R_{\text{acc}}(i) = \sigma \sqrt{\frac{8kT}{\pi\mu}} n(i) n_d,$$

where σ is the collision cross-section between the species *i* and the grain, $\sqrt{(8kT/\pi\mu)}$ is the relative average speed of the species *i* and the grain (k is the Boltzmann constant, μ is the reduced mass of the

species i and the grain, so mainly the mass of species i , $n(i)$ is the density of the species i , and n_d is the grain density.

For desorption from the surface, we consider thermal desorption and desorption induced by cosmic rays (Hasegawa & Herbst 1993; Dartois et al. 2015) as well as by exothermic chemical reactions (the exothermicity of surface chemical reactions allows for the species to be desorbed after their formation; Garrod, Wakelam & Herbst 2007). The Garrod et al. (2007) chemical desorption mechanism leads to approximately 1 per cent desorption of the newly formed species with 99 per cent remaining on the grain surfaces (this corresponds to an a factor of 0.01 in Garrod et al. 2007). The binding energies of species to the surface have been updated from Wakelam et al. (2017). These values are considered to be isotope independent as they are controlled through interactions that vary as a function of their electronic properties, which are identical for isotopologues, rather than as a function of the mass of the species.

The chemical composition of the gas phase and the grain surfaces is computed as a function of time. The gas and dust temperatures are equal to 10 K, the total H_2 density is equal to $2 \times 10^4 \text{ cm}^{-3}$ (various runs have been performed with the total H density varied between 2×10^4 and $2 \times 10^5 \text{ cm}^{-3}$). The cosmic ray ionization rate is equal to $1.3 \times 10^{-17} \text{ s}^{-1}$, and the total visual extinction (A_V) is set equal to 10. All elements are assumed to be initially in atomic form except for hydrogen, which is entirely molecular. Elements with an ionization potential below the maximum energy of ambient UV photons (13.6 eV, the ionization energy of H atoms) are initially in a singly ionized state, i.e. C, S, and Fe. The initial abundances shown in Table 2 are similar to those of table 1 of Hincelin et al. (2011), the C/O elemental ratio being equal to 0.7 in this study. In the nominal version of the model, sulphur is not depleted leading to better agreement with observations (Fuente et al. 2016; Vidal et al. 2017). However, a run was performed with a sulphur depletion factor of 10, allowing us to conclude that sulphur chemistry has a negligible effect on nitrogen fractionation. Dust grains are considered to be spherical with a $0.1 \mu\text{m}$ radius, a 3 g cm^{-3} density and about 10^6 surface sites, all chemically active. The dust to gas mass ratio is set to 0.01.

2.1 ^{15}N exchange reactions

In the ISM, some fractionation may occur due to the fact that zero-point energy (ZPE) differences favour one direction (reverse or forward) for barrierless exchange reactions (such as $^{15}\text{N}^+ + \text{N}_2 \rightarrow \text{N}^+ + ^{15}\text{NN}$). The rate constants for the fractionation reactions have been studied in detail (Terziewa & Herbst 2000; Roueff et al. 2015). Using the work of Henchman & Paulson (1989), we consider in this work that all reactions involve adduct formation that corresponds to reactions of type B in Roueff et al. (2015). Then (f = forward = reaction towards the right in Table 3, r = reverse = reaction towards the left in Table 3),

$$k_f = \alpha \times (T/300)^\beta \times f(\text{B}, m) / (f(\text{B}, m) + \exp(\Delta E/kT)),$$

$$k_r = \alpha \times (T/300)^\beta \times \exp(\Delta E/kT) / (f(\text{B}, m) + \exp(\Delta E/kT))$$

with α and β given by capture theory for barrierless reactions, $f(\text{B}, m)$ is related to the symmetry of the system (Terziewa & Herbst 2000), and ΔE = exothermicity of the reactions (see Table 3).

We checked that the $^{15}\text{N} + \text{HCNH}^+$ and $^{15}\text{N} + \text{N}_2\text{H}^+$ reactions have large barriers in the entrance valley as found by Roueff et al. (2015), so that these processes become negligibly small at low temperature. We searched for additional processes that could lead to nitrogen fractionation, although no efficient ones were found. This is due to the fact that nitrogen is mainly present as neutral N

atoms, which are reactive only with radicals (Dutuit et al. 2013) and a few ions; reactions having bimolecular exit channels leading to N_2 , CN, HCN, $\text{HCN}^+/\text{HNC}^+$, and HCNH^+ , which prevent efficient isotopic exchange. Among them, the $\text{HCNH}^+ + \text{HC}^{15}\text{N}$ and $\text{NH}_4^+ + ^{15}\text{NH}_3$ reactions favour nitrogen fractionation for HCNH^+ and NH_4^+ . However, in dense molecular clouds, the abundances of HCN and NH_3 are too low for these reactions to lead to significant fractionation. For the $\text{HCNH}^+ + \text{H}^{15}\text{NC}$ reaction, once the adduct is formed, the most exothermic exit channels will always be favoured, that is, $\text{HC}^{15}\text{NH}^+ + \text{HCN}$ and $\text{HCNH}^+ + \text{HC}^{15}\text{N}$ at equilibrium (both equal to 0.5 as the energy corresponds to the exothermicity of the $\text{HNC} \rightarrow \text{HCN}$ isomerization), so that this reaction does not induce nitrogen fractionation.

Roueff et al. (2015) proposed that the $\text{N} + \text{CN}$ reaction may play a role in nitrogen fractionation. Wirström & Charnley (2018) have shown that the inclusion of the $^{15}\text{N} + \text{CN} \rightarrow \text{N} + \text{C}^{15}\text{N}$ reaction leads to some ^{15}N enrichment in nitriles. However, considering the bimolecular exit channel of the $^{15}\text{N} + \text{CN}$ reaction (Daranlot et al. 2012), it is highly unlikely that this reaction leads to efficient ^{15}N fractionation.

On grains, exchange reactions are not efficient in our model because we consider that the addition or bimolecular channels dominate, for example, $s\text{-}^{15}\text{N} + s\text{-CN} \rightarrow s\text{-}^{15}\text{NCN}$, $s\text{-CN}^{15}\text{N}$ but not $s\text{-N} + s\text{-C}^{15}\text{N}$. As diffusion and tunnelling are mass dependent, they are not strictly equivalent for the various isotopologues. These effects are included in the model but they only have a small effect on ^{15}N fractionation.

2.2 $\text{HCNH}^+ + \text{electron}$

Electronic dissociative recombination (DR) of HCNH^+ is a very important pathway for CN, HCN, and HNC production. The experiments of Mendes et al. (2012) showed that the majority of the exothermic energy released by the $\text{HCNH}^+ + e^-$ reaction is carried away as internal energy of the HCN–HNC products. This is in good agreement with the fact that about 30 per cent of the HCN–HNC produced dissociates into $\text{CN} + \text{H}$. In interstellar clouds, the only way to relax this internal energy is through radiative emission of an infrared photon. As noted by Herbst, Terziewa & Talbi (2000), the typical time-scales for HNC–HCN interconversion is much shorter than relaxation by one infrared photon. Consequently, as relaxation occurs slowly, isomerization leads to balanced isomeric abundances at each internal energy. The final balance is determined at or near the effective barrier to isomerization, which corresponds to the energy of the transition state. The ratio between the isomeric forms is then approximated by the ratio of the ro-vibrational densities of states of the isomers at the isomerization barrier. Statistical theory leads to a HCN/HNC ratio close to 1 for the main isotopologues (Herbst et al. 2000). This result has been confirmed by Barger, Wodtke & Bowman (2003) through ab initio calculations of the radiative relaxation of HCN–HNC at energies above the barrier. Assuming a branching ratio of 1 for the main isotopologue production HCN/HNC, statistical theory leads to a branching ratio equal to 0.91 for $\text{HC}^{15}\text{N}/\text{H}^{15}\text{NC}$ considering the variation in the ro-vibrational densities of states, the branching ratio for CN production being the same for all isotopologues.

3 RESULTS

The time-dependent abundances of the gas-phase species N_2H^+ , NH_3 , $s\text{-NH}_3$, HCN, HNC, CN, HC_3N , CH_3CN , and H_2CN (relative to H_2) calculated by our model are shown in Fig. 1.

Table 1. Observations for ^{15}N in dense molecular clouds (we include the measurements where the main isotopologue emission lines show small opacity, but the cases where the main isotopologue emission lines show very strong opacity or the ones using the double isotopes methods are not reported here in most of the measurements). The values given in brackets are errors reported in the literature, which may be strongly underestimated.

Species	Ratio	Cloud	References
$\text{N}_2\text{H}^+ / ^{15}\text{NNH}^+$	1000^{+260}_{-220}	L1544	(Redaelli et al. 2018)
	> 600	B1	(Daniel et al. 2013)
	320(60)	OMC-2	(Kahane et al. 2018)
	700^{+210}_{-140}	L694-2	(Redaelli et al. 2018)
$\text{N}_2\text{H}^+ / \text{N}^{15}\text{NH}^+$	920^{+300}_{-200}	L1544	(Redaelli et al. 2018)
	400^{+100}_{-65}	B1	(Daniel et al. 2013)
	330^{+170}_{-100}	L16293E	(Daniel et al. 2016)
	240(50)	OMC-2	(Kahane et al. 2018)
	670^{+150}_{-230}	L183	(Redaelli et al. 2018)
	730(250)	L429	(Redaelli et al. 2018)
$\text{NH}_3 / ^{15}\text{NH}_3$	580^{+140}_{-110}	L694-2	(Redaelli et al. 2018)
	330(50)	B1	(Lis et al. 2010)
$\text{CN} / \text{C}^{15}\text{N}$	300^{+55}_{-40}	B1	(Daniel et al. 2013)
	240^{+135*}_{-65}	B1	(Daniel et al. 2013)
$\text{HCN} / \text{HC}^{15}\text{N}$	$270(60)^*$	OMC-2	(Kahane et al. 2018)
	165^{+30**}_{-25}	B1	(Daniel et al. 2013)
$\text{HNC} / \text{H}^{15}\text{NC}$	$338(28)^*$	L1498	(Magalhães et al. 2018)
	75^{+25**}_{-15}	B1	(Daniel et al. 2013)
$\text{HNC} / \text{H}^{15}\text{NC}$	$250\text{-}330^*$	TMC1	(Liszt & Ziurys 2012)
	$\text{HC}_3\text{N} / \text{HC}_3^{15}\text{N}$	257(54)	TMC1
$\text{HC}_3\text{N} / \text{HC}_3^{15}\text{N}$	338(12)	L1527	(Araki et al. 2016)
	400(20)	L1544	(Hily-Blant et al. 2018)
	344(53)	TMC1	(Taniguchi & Saito 2017)

:main isotopologue shows opacity.

:main isotopologue shows very strong opacity.

Table 2. Elemental abundance ($/\text{H}$).

Element	Abundance
He	0.09
C	$1.7\text{e-}4$
N (^{14}N)	$6.2\text{e-}5$
^{15}N	$1.406\text{e-}7$
$^{14}\text{N}/^{15}\text{N}$	441
	300
O	$2.4\text{e-}4$
S	$1.5\text{e-}5$
Fe	$1.00\text{e-}8$

Good agreement is obtained when our calculations are compared with the observed fractional abundances of the main isotopologues of HCN, HNC, and CN (and many other species such as NO, CH, C_2H , $c\text{-C}_3\text{H}_2$, ...) for typical dense molecular clouds with a cloud age around $(3\text{--}6) \times 10^5$ yr for a total density $n(\text{H}_2) = 2 \times 10^4 \text{ cm}^{-3}$ (the observed abundances shown in Fig. 1 are those derived for TMC-1 molecular cloud; Crutcher, Churchwell & Ziurys 1984; Ohishi et al. 1994; Dickens et al. 1997; Pratap et al. 1997; Turner, Terzieva & Eric 1999; Gratier et al. 2016). The agreement is a little less good for NH_3 , N_2H^+ , HC_3N , CH_3CN , and H_2CN , reflecting our poorer understanding of nitrogen chemistry in dense molecular clouds. The underestimation of NH_3 , HC_3N , and CH_3CN , with regards to previous versions of our model (Loison et al. 2014a,b), are partly due to the introduction of the reactions with atomic carbon that have been recently measured for $\text{C} + \text{NH}_3$ (Bourgalais et al. 2015; Hickson et al. 2015) and calculated for $\text{C} + \text{HC}_3\text{N}$

(Li et al. 2006). The overestimation of H_2CN may be due to an overestimation of the rate for the $\text{N} + \text{CH}_3$ reaction at 10 K, the main source of H_2CN (Hébrard et al. 2012). The rate constant for this reaction could decrease at low temperature (Marston et al. 1989), so this process should be re-investigated at even lower temperatures.

The time-dependent $^{14}\text{N}/^{15}\text{N}$ ratios calculated by our model for the main nitrogen compounds in the gas phase are shown in Fig. 2.

Our model leads to low nitrogen fractionation levels. This result demonstrates that neither gas-phase isotopic exchange reactions (see Table 3) nor diffusion on grains have significant effects on nitrogen fractionation in dense interstellar clouds. Although the overall fractionation levels are low, certain results should be highlighted. First, the lower $^{14}\text{N}/^{15}\text{N}$ ratios for HNC derived from the DR of HCNH^+ , a reaction leading to more ^{15}N enrichment for HNC than for HCN and CN as explained in the model description section. Another nitrogen fractionation pathway occurs through mass-dependent accretion. Here, the accretion time for each isotopologue of a given species is dependent on its mass, so that in the case of atomic nitrogen, ^{14}N will be removed slightly more quickly from the gas phase than ^{15}N . Assuming an initial elemental $^{14}\text{N}/^{15}\text{N}$ ratio in the local ISM equal to 441, for a typical cloud age around $3\text{--}6 \times 10^5$ yr and a total density of $n(\text{H}_2) = 2 \times 10^4 \text{ cm}^{-3}$, the model leads to some nitrogen fractionation, with $^{14}\text{N}/^{15}\text{N}$ ratios around 400 for most of the species (N_2H^+ , NH_3 , HCN, CN, ...) and 360 for HNC. This depletion-induced fractionation effect for nitrogen is only efficient because atomic nitrogen is relatively unreactive in the gas phase (Daranlot et al. 2011, 2012, 2013), so that sticking on to grains is the dominant loss process. Although the difference of the accretion rate between ^{14}N and ^{15}N is small,

Table 3. Review of reactions involved in ^{15}N fractionation.

	Reaction		α	β	$\Delta E(\text{K})$	$f(\text{B,m})$	Reference
1.	$^{15}\text{N}^+ + \text{H}_2$	$\leftarrow ^{15}\text{NH}^+ + \text{H}$	4.2e-10	0	37.1	–	(Marquette, Rebrion & Rowe 1988; Roueff et al. 2015)
2.	$\text{H} + ^{15}\text{NNH}^+$	$\leftarrow \text{N}^{15}\text{NH}^+ + \text{H}$	‘0’	–	–8.1	–	Barrier of 1500 K at M06-2X/VTZ level (this work, see Appendix)
3.	$^{15}\text{N} + \text{NNH}^+$	$\leftarrow ^{15}\text{NNH}^+ + \text{N}$	‘0’	–	–	–	Large barrier, see Roueff et al. (2015)
4.	$^{15}\text{N} + \text{NNH}^+$	$\leftarrow \text{N}^{15}\text{NH}^+ + \text{N}$	‘0’	–	–	–	Large barrier, see Roueff et al. (2015)
5.	$^{15}\text{N} + \text{HCNH}^+$	$\leftarrow \text{HC}^{15}\text{NH}^+ + \text{N}$	‘0’	–	–	–	Large barrier, see Roueff et al. (2015)
6.	$^{15}\text{N} + \text{CN}$	$\leftarrow \text{C} + ^{15}\text{NN}$	8.8e-11	0.42	–	–	(Daranlot et al. 2012)
	$\leftarrow \text{N} + \text{C}^{15}\text{N}$	–	0	–	–	–	See text
7.	$^{15}\text{N}^+ + \text{N}_2$	$\leftarrow \text{N}^+ + \text{N}^{15}\text{N}$	3.3e-10	0	–28.3	2	(Fehsenfeld et al. 1974; Anicich, Huntress & Futrell 1977)
8.	$\text{N}^{15}\text{N} + \text{N}_2\text{H}^+$	$\leftarrow \text{N}^{15}\text{NH}^+ + \text{N}_2$	4.6e-10	0	–10.3	0.5	(Adams & Smith 1981)
9.	$\text{N}^{15}\text{N} + \text{N}_2\text{H}^+$	$\leftarrow ^{15}\text{NNH}^+ + \text{N}_2$	2.3e-10	0	–2.1	0.5	(Adams & Smith 1981)
10.	$\text{N}^{15}\text{N} + ^{15}\text{NNH}^+$	$\leftarrow \text{N}^{15}\text{NH}^+ + \text{N}^{15}\text{N}$	2.3e-10	0	–8.1	1	(Adams & Smith 1981)
11.	$\text{NH}_4^+ + ^{15}\text{NH}_3$	$\leftarrow ^{15}\text{NH}_4^+ + \text{NH}_3$	1.3e-9	–0.5	–14.5	1	This work (capture rate constant assuming no barrier for proton exchange)
12.	$\text{HCNH}^+ + \text{HC}^{15}\text{N}$	$\leftarrow \text{HC}^{15}\text{NH}^+ + \text{HCN}$	2.0e-9	–0.5	–10.1	1	This work based on (Cotton, Francisco & Klemperer 2013)
13.	$\text{HCNH}^+ + \text{H}^{15}\text{NC}$	$\leftarrow \text{HC}^{15}\text{NH}^+ + \text{HCN}$	1.0e-9	–0.5	0	–	This work based on (Cotton et al. 2013)
	$\leftarrow \text{HCNH}^+ + \text{HC}^{15}\text{N}$	1.0e-9	–0.5	0	–	–	–
14.	$\text{HCNH}^+ + \text{e}^-$	$\leftarrow \text{HCN} + \text{H}$	9.62e-8	–0.65	0	–	Rate constant from (Semaniak et al. 2001)
	$\leftarrow \text{HNC} + \text{H}$	–	9.62e-8	–0.65	0	–	Branching ratios from (Herbst et al. 2000; Barger et al. 2003; Mendes et al. 2012)
15.	$\leftarrow \text{CN} + \text{H} + \text{H}$	–	9.06e-8	–0.65	0	–	–
	$\text{HC}^{15}\text{NH}^+ + \text{e}^-$	$\leftarrow \text{HC}^{15}\text{N} + \text{H}$	9.34e-8	–0.65	0	–	This work (see text)
	$\leftarrow \text{H}^{15}\text{NC} + \text{H}$	–	9.90e-8	–0.65	0	–	–
	$\leftarrow \text{C}^{15}\text{N} + \text{H} + \text{H}$	–	9.06e-8	–0.65	0	–	–

Notes. $k_f = \alpha \times (T/300)^\beta \times f(\text{B,m}) / (f(\text{B,m}) + \exp(\Delta E/kT))$,

$k_r = \alpha \times (T/300)^\beta \times \exp(\Delta E/kT) / (f(\text{B,m}) + \exp(\Delta E/kT))$.

the effect is large enough to remove a few tens of percent more ^{14}N atoms from the gas phase when the accretion time reaches 4×10^5 yr. As the remaining atomic nitrogen in the gas phase is depleted in ^{14}N , all nitrogen-bearing species formed through gas-phase chemistry will reflect these higher ^{15}N levels with various values depending on the individual formation mechanisms (such as $\text{N} + \text{CH} \rightarrow \text{CN} + \text{H}$ for example). Although the calculated $^{14}\text{N}/^{15}\text{N}$ values for NH_3 , HCN , HNC , CN , and HC_3N are lower than those obtained in earlier models, they are still above the observed values shown in Table 1. The effect is not very large for evolved clouds because for cloud chemical ages in the range $3\text{--}6 \times 10^5$ yr, most of the nitrogen has already been removed from the gas phase. So, even if the gas phase is depleted in ^{14}N , the $^{14}\text{N}/^{15}\text{N}$ fraction for species formed on grains is close to or slightly above the elemental $^{14}\text{N}/^{15}\text{N}$ ratio in the local ISM. Desorption mechanisms will release ^{14}N -bearing molecules back into the gas phase resulting in a reduction in the gas-phase fractionation levels for these species.

Besides the uncertainties generated by the desorption mechanisms, grain depletion is the most efficient fractionation process in our model. This leads to lower $^{14}\text{N}/^{15}\text{N}$ ratios for species formed in the gas phase in dense molecular clouds (CN , HCN , HNC) than the solar wind reference value (441 ± 2.5 ; Marty et al. 2010) corresponding to the nitrogen reservoir of the pre-stellar cloud. However, mass-dependent sticking rate cannot explain $^{14}\text{N}/^{15}\text{N}$ ratios as low as those listed in Table 1, except when larger uncertainties than those reported in the literature are considered. Nevertheless, considering a lower initial elemental $^{14}\text{N}/^{15}\text{N}$ ratio in the local ISM, around 300 from Romano et al. (2017), the inclusion

of mass-dependent accretion for N atoms results in agreement with most observations for CN , HCN , HNC , HC_3N , and NH_3 (except HCN and HNC in B1 and HC_3N in L1544, values shown in Table 1), the average for all these observations being equal to 312 ± 48 , but also for HC_5N (Taniguchi & Saito 2017).

The comparison with previous studies is not obvious due to the large differences between models. The low nitrogen fractionation induced by chemistry is similar in Roueff et al. (2015), despite the large differences in models (no grain chemistry in Roueff et al. 2015) and substantial differences in the chemical networks. The low fractionation is due in both cases to the absence of efficient fractionation reactions. Wirström & Charnley (2018) found some nitrogen fractionation in their recent work. In their model, NH_3 in the gas phase shows some ^{15}N depletion due to specific reactions of $^{15}\text{N}^+$ in conjunction with a large gas-phase N_2 abundance. The large N_2 abundance is due to the fact that Wirström & Charnley (2018) consider that N and N_2 do not freeze out, which is not the case in our model. They also found some ^{15}N enrichment in CN and HCN due to the $^{15}\text{N} + \text{CN}$ reaction. However, this reaction is likely to be inefficient (see Section 2.1). Moreover, as N atom grain depletion is not considered by these authors, the $^{14}\text{N}/^{15}\text{N}$ mass-dependent accretion rate cannot be reproduced. In their recent study, Furuya & Aikawa (2018) developed a full gas-grain model for ^{15}N fractionation including the first step of dense molecular cloud formation where UV photons can penetrate. They obtained some ^{15}N fractionation due essentially to the isotope-selective photodissociation of N_2 , whereas chemistry is inefficient. As we consider $A_v = 10$ in our study, we cannot reproduce such

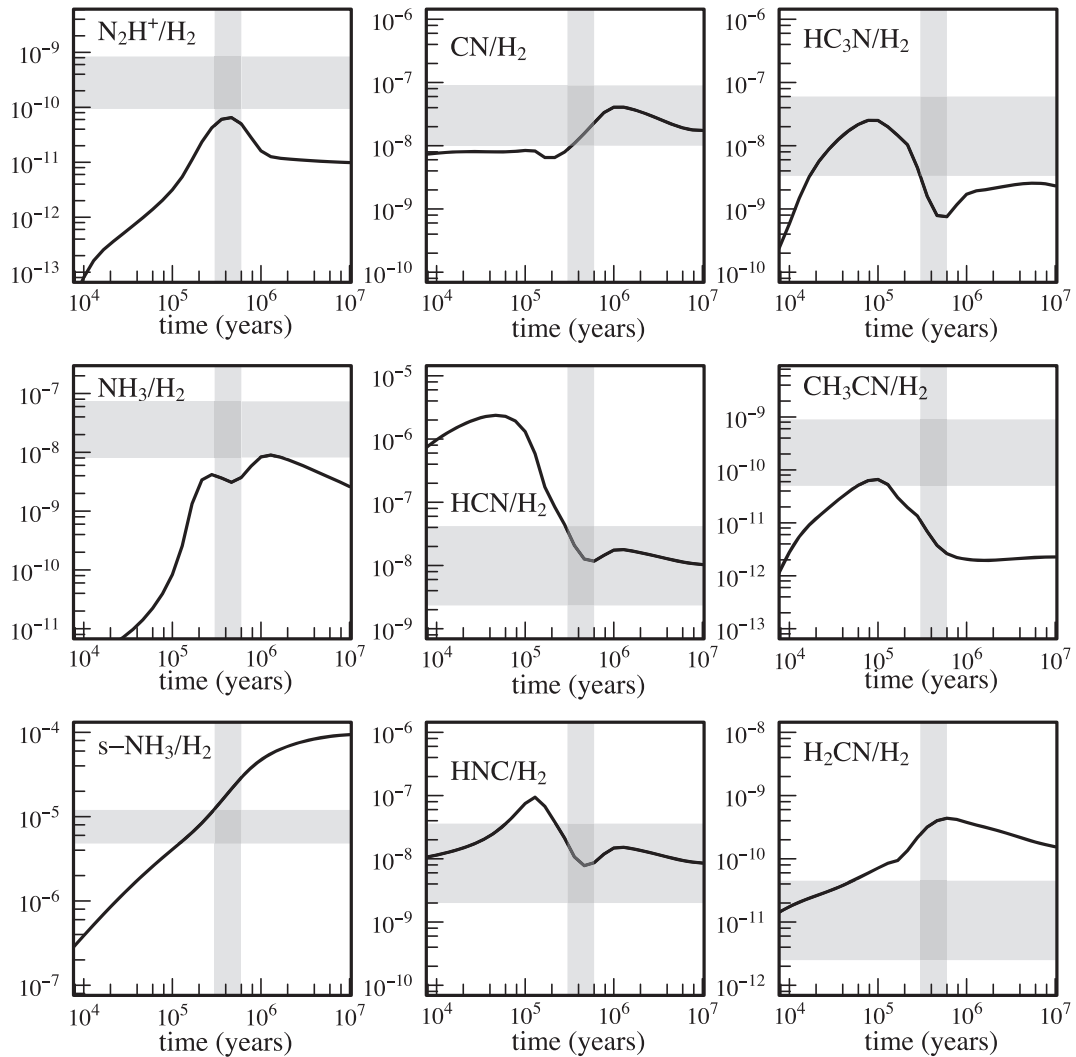


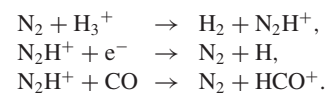
Figure 1. Gas phase species abundances (relative to H_2) of N_2H^+ , NH_3 , $s\text{-NH}_3$, HCN , HNC , CN , HC_3N , CH_3CN , and H_2CN studied in this work as a function of time predicted by our model for $\text{N}(\text{H}_2) = 2 \times 10^4 \text{ cm}^{-3}$ and $T = 10 \text{ K}$. The horizontal grey rectangles represent the abundances observed for TMC-1 (Crutcher et al. 1984; Ohishi et al. 1994; Dickens et al. 1997; Pratap et al. 1997; Turner et al. 1999; Gratier et al. 2016) and (Boogert, Gerakines & Whittet 2015) for $s\text{-NH}_3$ on Ice (light young stellar objects), including uncertainties. The vertical grey rectangles represent the TMC-1 cloud age given by the best agreement between the abundances given by our model and the observations (N_2H^+ , NH_3 , HCN , HNC , CN , HC_3N , CH_3CN but also NO , CH , C_2H , $c\text{-C}_3\text{H}_2$, ...).

effects. In their work, they consider the difference in the adsorption rates for ^{14}N and ^{15}N . However, in their model this effect is likely to be significantly smaller than the ^{15}N atomic enrichment in the gas phase due to the photodissociation of N^{15}N . This is because N is depleted on to grains when A_v is in the 0–2 range, where isotope-selective photodissociation of N_2 is at work and very efficient.

3.1 $^{15}\text{NNH}^+$, N^{15}NH^+ fractionation

Our model produces similar low ^{15}N fractionation effects for N-bearing species formed by gas-phase reactions. Simulated isotopologue abundances for N_2H^+ show that fractionation levels are small and incompatible with observations in L1544 (Redaelli et al. 2018). Little enrichment occurs for N_2H^+ in our model as the exchange reaction $\text{N}^{15}\text{N} + \text{N}_2\text{H}^+ \rightarrow \text{N}^{15}\text{NH}^+/\text{N}^{15}\text{NH}^+ + \text{N}_2$ is inefficient due to its low exothermicity. In addition, the DR reaction of N_2H^+ and its reaction with CO are much more efficient sinks of N_2H^+ . It should

be noted that with our model, both N^{15}NH^+ and $^{15}\text{NNH}^+$ have very similar low ^{15}N fractionation levels. Specifically, the $\text{N}^{15}\text{N} + \text{NNH}^+ \rightarrow \text{NN} + \text{N}^{15}\text{NH}^+/\text{N}^{15}\text{NNH}^+$ reactions are inefficient despite large rate constant at 10 K because the flux of these reactions is negligibly small compared to the fluxes of DR and the reaction with CO . The chemistry of N_2H^+ is essentially driven by three main reactions:



As the $\text{N}_2 + \text{H}_3^+$ and $\text{N}_2\text{H}^+ + \text{CO}$ reactions are direct barrierless processes, they should not be affected by the ZPE difference of any of the N_2H^+ isotopologues. In our model, we assume that the rate constants for DR of $^{15}\text{NNH}^+$, N^{15}NH^+ , and N_2H^+ are identical. However, Lawson, Osborne & Adams (2011) showed that the DR of N_2H^+ , $^{15}\text{N}_2\text{H}^+$, and N_2D^+ have notable differences (more than

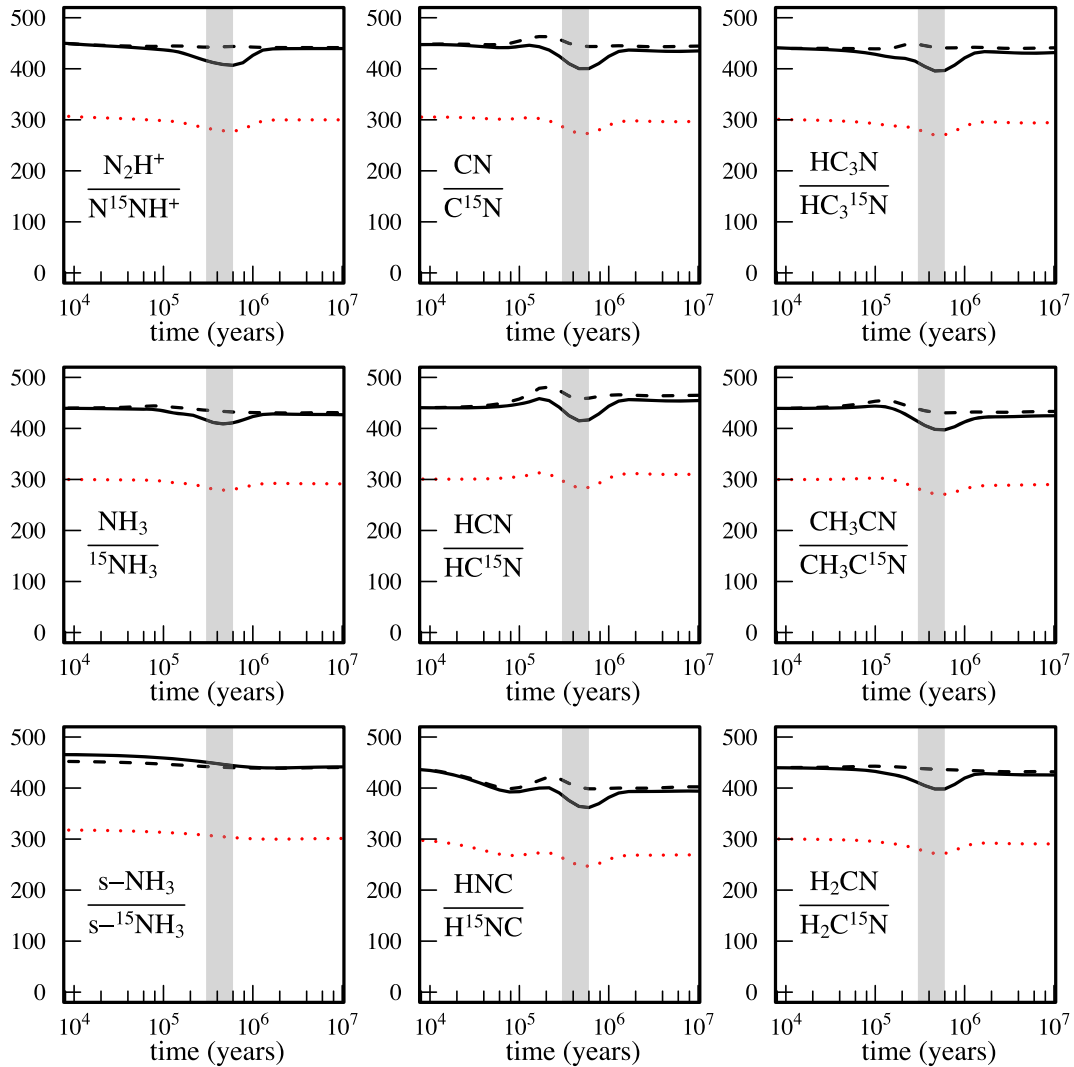


Figure 2. Calculated $N/^{15}N$ ratio for the main nitrogen species in the gas phase as a function of time predicted by our model ($N(H_2) = 2 \times 10^4 \text{ cm}^{-3}$, $T = 10 \text{ K}$; for an elemental $N/^{15}N$ ratio equal to 441 in continuous black lines, and equal to 300 in the red dotted lines). With our model, both $N^{15}NH^+$ and $^{15}NNH^+$ have very similar ^{15}N fractionation levels. In the black dashed lines, model with the same sticking rate constant for all isotopologues of a given species (same rate constant for N_2 and $N^{15}N$, ...) for an elemental $N/^{15}N$ ratio equal to 441. The vertical grey rectangles represent the TMC-1 cloud age as described in Fig. 1.

20 per cent) between 300 and 500 K, the DR reaction of N_2H^+ being more efficient than the DR reactions of $^{15}N_2H^+$ and N_2D^+ . However, that result does not necessarily mean that the DR reactions of $N^{15}NH^+$ and $^{15}NNH^+$ are less efficient than N_2H^+ at low temperature due to their complexity. Indeed, the difference in ZPE may favour intercrossing curves between the ions and neutral for $^{15}NNH^+$ and $N^{15}NH^+$ leading to an unexpected increase at low temperature. Experimental measurements of the DR rates of $^{15}NNH^+$ and $N^{15}NH^+$ are clearly needed but higher DR rate constants for $N^{15}NH^+$ and $^{15}NNH^+$ than the equivalent N_2H^+ ones could be possible. If the DR reactions of $N^{15}NH^+$ and $N^{15}NH^+$ are more efficient than the N_2H^+ one, the $N_2H^+/N^{15}NH^+$ and $N_2H^+/^{15}NNH^+$ ratios will increase above and beyond the input nitrogen isotope ratio value. When gas-phase CO is low, the main loss for N_2H^+ is DR. Then, if the rate constants for the DR of $^{15}NNH^+$ and $N^{15}NH^+$ are more efficient than the DR of N_2H^+ , the $N_2H^+/^{15}NNH^+$ and $N_2H^+/N^{15}NH^+$ ratios are notably larger than the elemental $N/^{15}N$

ratio, around 900 for the conditions used in Fig. 3. However, when the CO abundance is large, the $N_2H^+ + CO$ reaction is competitive with DR and the $N_2H^+/^{15}NNH^+$ and $N_2H^+/N^{15}NH^+$ ratios are closer to the elemental $N/^{15}N$ ratio, namely around 620 for the conditions used in Fig. 3. It should be noted that this effect is highly dependent on the rate constants of the DR reactions of N_2H^+ , $^{15}NNH^+$, and $N^{15}NH^+$ in addition to the value of the rate constant for the $N_2H^+ + CO$ reaction measured only once (Bohme, Mackay & Schiff 1980) as well as the total density of the molecular cloud.

An interesting observation that supports this hypothesis is the evolution of the abundance ratios $N_2H^+/N^{15}NH^+$, $N_2H^+/N^{15}NH^+$, and N_2H^+/N_2D^+ towards various high-mass star-forming cores (Fontani et al. 2015). In these regions, the $N_2H^+/N^{15}NH^+$ and $N_2H^+/N^{15}NH^+$ ratios are seen to increase with the mass of the core, while the corresponding N_2H^+/N_2D^+ ratio, whose value is known to be a good indicator of the level of CO depletion (Roberts,

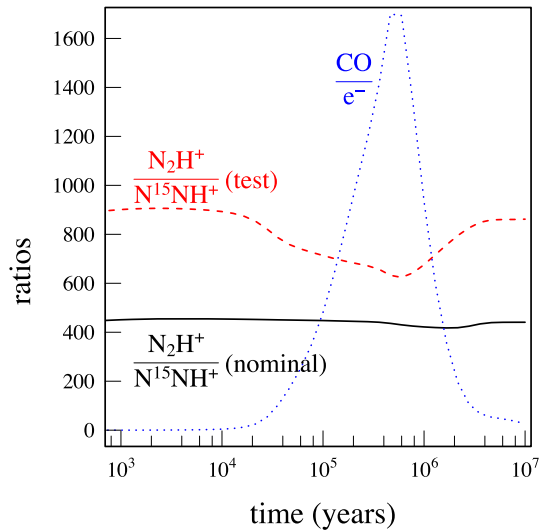


Figure 3. Calculated $\text{N}_2\text{H}^+/\text{N}^{15}\text{NH}^+$ ratios for the nominal model (continuous black line) and considering a N_2H^+ DR rate constant divided by 2 (test, dashed red line), $n(\text{H}_2) = 2 \times 10^4 \text{ cm}^{-3}$, $T = 10 \text{ K}$. The CO/e^- ratio (dotted blue lines) is also plotted showing that when CO abundance reaches its maximum, the $\text{CO} + \text{N}_2\text{H}^+$ reaction become competitive with the $\text{N}_2\text{H}^+ + e^-$ reaction.

Herbst & Millar 2003; Crapsi et al. 2005), is seen to decrease for the same objects.

4 CONCLUSIONS

Despite a thorough search initiated in Roueff et al. (2015) and continued in this work, chemistry does not appear to lead to significant nitrogen fractionation. The most efficient fraction processes are the mass-dependent fractionation mechanism induced by depletion on to grains and DR of HCNH^+ , although these effects produce relatively low fractionation levels. This low nitrogen fractionation may not be incompatible with observations. Considering the uncertainties brought about by saturation of the main isotopologues transitions, nitrogen fractionation in dense molecular clouds may not be so different to the ‘elemental’ $^{14}\text{N}/^{15}\text{N}$ ratio in the local ISM, of approximately 300 (Ade & Ziurys 2012). Indeed, apart from N_2H^+ , all other nitrogen compounds (CN, HCN, HNC, HC_3N , and NH_3 , described in Table 1 and HC_5N in Taniguchi & Saito 2017) seem to show similar nitrogen fractionation levels in dense molecular clouds, namely 312 ± 48 from values in Table 1 (without all N_2H^+ observations nor those for HCN and HNC in B1). The difference between the ‘elemental’ $^{14}\text{N}/^{15}\text{N}$ ratio in the local ISM and the solar wind reference value, 441 ± 5 (Marty et al. 2010), being in that case explained through galactic chemical evolution (Romano et al. 2017). However, this scenario cannot explain the observed HC_5N fractionation in L1544 (400 ± 20 ; Hily-Blant et al. 2018), neither can it explain the strong observed enrichment in HCN and HNC in B1 (Daniel et al. 2013). Additionally, different dissociative DR rates are required to explain the observed N_2H^+ fractionation levels, which need experimental confirmation. Moreover, Colzi et al. (2018) recently found a $^{14}\text{N}/^{15}\text{N}$ ratio for HCN and HNC across the galaxy much closer to 400, which challenges the currently adopted $^{14}\text{N}/^{15}\text{N}$ ratio value of 300 in the local ISM.

An alternative scenario to explain nitrogen fractionation in dense molecular clouds involves N_2 photodissociation. Indeed, N_2 photodissociation is the only efficient process leading to significant ^{15}N enrichment in a wide range of astrochemical environments such as protoplanetary discs, comets, and planetary atmospheres (Liang et al. 2007; Li et al. 2013; Heays et al. 2014; Dobrijevic & Loison 2018). However, to be efficient, isotope-selective N_2 photodissociation requires a large N_2 column density in conjunction with low A_v . Furuya & Aikawa (2018) developed a model where N_2 and N^{15}N photodissociation in translucent molecular clouds (with low visual extinction) at the outset of molecular cloud formation can induce nitrogen fractionation. In the translucent part of the molecular clouds, N_2 becomes ^{15}N depleted, while CN, HCN, HNC, and NH_3 become ^{15}N enriched. The N^{15}N depletion is partly conserved in dense molecular cloud but their model cannot reproduce the high ^{15}N depletion of N_2H^+ observed in L1544 and L429 (Redaelli et al. 2018). Moreover, the ^{15}N enrichment is not conserved in the gas phase of dense molecular clouds because N atoms are efficiently transformed into s- NH_3 on ices, which becomes the main ^{15}N reservoir. As s- NH_3 is not easily desorbed, most of the gas-phase nitrogen chemistry in the dense molecular clouds is initiated by N_2 dissociation (through cosmic rays or through its reaction with He^+). As N_2 is depleted in ^{15}N , the chemistry induced by N_2 dissociation in the dense clouds counterbalances the enrichment due to N_2 photodissociation in the translucent cloud. Then, the Furuya & Aikawa (2018) model requires low elemental ^{15}N fractionation levels in the local ISM to reproduce the observations. The s- NH_3 trapping effect is very efficient in the Furuya & Aikawa (2018) work because NH_3 photodesorption is inefficient and chemical desorption was fixed to 1 per cent following Garrod et al. (2007). However, this amount can be much higher in addition to atoms and small species as shown by Minissale et al. (2016). Then, the rapid hydrogenation of s-N, s-NH, and s- NH_2 may lead to much higher NH, NH_2 , and NH_3 abundances in the gas phase. Additionally, the photodissociation of s- NH_3 , followed by the s-H + s- NH_2 and s-H + s-NH reactions ($\text{NH} + \text{H} + \text{H}$ are the favoured products for NH_3 photodissociation at 121.6 nm; Slinger & Black 1982), may strongly enhance chemical desorption through cycling processes. Then, s- NH_3 may not be such an important reservoir, and the release of NH_2 and NH_3 in the gas phase (with NH_2 and NH_3 enriched in ^{15}N) may induce an efficient nitrogen chemistry, potentially much more efficient than the one induced by N_2 dissociation. A particularly interesting aspect of the Furuya & Aikawa (2018) model is that it may explain variable ^{15}N fractionation levels from cloud to cloud depending on the formation history.

Our model clearly demonstrates that chemistry cannot lead to high nitrogen fractionation levels but there remains much work to be done to clarify the nitrogen fractionation issue from diffuse clouds to the Solar system. Among these issues, an in-depth review of the various observations is required to assess the dispersion of nitrogen fractionation data. Also, DR rates for the various N_2H^+ isotopologues need to be measured. Finally, a full molecular cloud formation model such as the one developed by Furuya & Aikawa (2018) seems to be an indispensable approach for the future, requiring, however, better characterization of critical processes such as chemical desorption.

ACKNOWLEDGEMENTS

This work was supported by the program ‘Physique et Chimie du Milieu Interstellaire’ (PCMI) funded by CNRS and CNES. VW researches are funded by the ERC Starting Grant (3DICE,

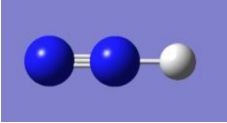
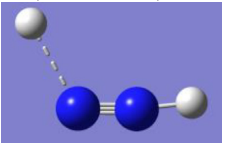
grant agreement 336474). Computer time was provided by the Pôle Modélisation HPC facilities of the Institut des Sciences Moléculaires UMR 5255 CNRS – Université de Bordeaux, co-funded by the Nouvelle Aquitaine region.

REFERENCES

- Adams N. G., Smith D., 1981, *ApJ*, 247, L123
- Adande G. R., Ziurys L. M., 2012, *ApJ*, 744, 194
- Anicich V. G., Huntress W. T., Jr, Futrell J. H., 1977, *Chem. Phys. Lett.*, 47, 488
- Araki M., Takano S., Sakai N., Yamamoto S., Oyama T., Kuze N., Tsukiyama K., 2016, *ApJ*, 833, 291
- Barger T., Wodtke A. M., Bowman J. M., 2003, *ApJ*, 587, 841
- Bohme D. K., Mackay G. I., Schiff H. I., 1980, *J. Chem. Phys.*, 73, 4976
- Boogert A. C. A., Gerakines P. A., Whittet D. C. B., 2015, *ARA&A*, 53, 541
- Bourgais J. et al., 2015, *ApJ*, 812, 106
- Colzi L., Fontani F., Rivilla V. M., Sanchez-Monge A., Testi L., Beltran M. T., Caselli P., 2018, *MNRAS*, 478, 3693
- Cotton E. C., Francisco J. S., Klemperer W., 2013, *J. Chem. Phys.*, 139, 014304
- Crapsi A., Caselli P., Walmsley C. M., Myers P. C., Tafalla M., Lee C. W., Bourke T. L., 2005, *ApJ*, 619, 379
- Crutcher R. M., Churchwell E., Ziurys L. M., 1984, *ApJ*, 283, 668
- Daniel F. et al., 2013, *A&A*, 560, A3
- Daniel F. et al., 2016, *A&A*, 592, A45
- Daranlot J. et al., 2011, *Science*, 334, 1538
- Daranlot J., Hincelin U., Bergeat A., Costes M., Loison J. C., Wakelam V., Hickson K. M., 2012, *Proc. Natl. Acad. Sci.*, 109, 10233
- Daranlot J. et al., 2013, *Phys. Chem. Chem. Phys.*, 15, 13888
- Dartois E. et al., 2015, *A&A*, 576, A125
- Dickens J. E., Irvine W. M., DeVries C. H., Ohishi M., 1997, *ApJ*, 479, 307
- Dobrijevic M., Loison J. C., 2018, *Icarus*, 307, 371
- Dutuit O. et al., 2013, *ApJS*, 204, 20
- Fehsenfeld F. C., Albritton D. L., Bush Y. A., Fournier P. G., Govers T. R., Fournier J., 1974, *J. Chem. Phys.*, 61, 2150
- Fontani F., Caselli P., Palau A., Bizzocchi L., Ceccarelli C., 2015, *ApJ*, 808, L46
- Fuente A. et al., 2016, *A&A*, 593, A94
- Füri E., Marty B., 2015, *Nat. Geosci.*, 8, 515
- Furuya K., Aikawa Y., 2018, *ApJ*, 857, 105
- Garrod R. T., Wakelam V., Herbst E., 2007, *A&A*, 467, 1103
- Gerin M., Marcelino N., Biver N., Roueff E., Coudert L. H., Elkeurti M., Lis D. C., Bockelée-Morvan D., 2009, *A&A*, 498, L9
- Gonzalez-Alfonso E., Cernicharo J., 1993, *A&A*, 279, 506
- Gratier P., Majumdar L., Ohishi M., Roueff E., Loison J. C., Hickson K. M., Wakelam V., 2016, *ApJS*, 225, 25
- Hasegawa T. I., Herbst E., 1993, *MNRAS*, 261, 83
- Heays A. N., Visser R., Gredel R., Ubachs W., Lewis B. R., Gibson S. T., van Dishoeck E. F., 2014, *A&A*, 562, A61
- Hébrard E., Dobrijevic M., Loison J. C., Bergeat A., Hickson K. M., 2012, *A&A*, 541, A21
- Henchman M., Paulson J. F., 1989, *J. Chem. Soc. Faraday Trans. II*, 85, 1673
- Herbst E., Terzieva R., Talbi D., 2000, *MNRAS*, 311, 869
- Hickson K. M., Loison J. C., Bourgalais J., Capron M., Le Picard S. D., Goulay F., Wakelam V., 2015, *ApJ*, 812, 107
- Hily-Blant P., Faure A., Vastel C., Magalhães V., Lefloch B., Bachiller R., 2018, *MNRAS*, 480, 1174
- Hincelin U., Chang Q., Herbst E., 2015, *A&A*, 574, A24
- Hincelin U., Wakelam V., Hersant F., Guilloteau S., Loison J. C., Honvault P., Troe J., 2011, *A&A*, 530, A61
- Kahane C., Al-Edhari A. J., Ceccarelli C., López-Sepulcre A., Fontani F., Kama M., 2018, *ApJ*, 852, 130
- Lawson P. A., Osborne D., Jr, Adams N. G., 2011, *Int. J. Mass Spectrom.*, 304, 41
- Li H. Y. et al., 2006, *J. Chem. Phys.*, 124, 44307
- Li X., Heays A. N., Visser R., Ubachs W., Lewis B. R., Gibson S. T., van Dishoeck E. F., 2013, *A&A*, 555, A14
- Liang M. C., Heays A. N., Lewis B. R., Gibson S. T., Yung Y. L., 2007, *ApJ*, 664, L115
- Lis D. C., Wootten A., Gerin M., Roueff E., 2010, *ApJ*, 710, L49
- Liszt H. S., Ziurys L. M., 2012, *ApJ*, 747, 55
- Loison J. C., Wakelam V., Hickson K. M., Bergeat A., Mereau R., 2014a, *MNRAS*, 437, 930
- Loison J. C., Hickson K. M., Wakelam V., 2014b, *MNRAS*, 443, 398
- Loison J. C. et al., 2016, *MNRAS*, 456, 4101
- Loison J. C. et al., 2017, *MNRAS*, 470, 4075
- Lucas R., Liszt H., 1998, *A&A*, 337, 246
- Magalhães V. S., Hily-Blant P., Faure A., Hernandez-Vera M., Lique F., 2018, *A&A*, 615, A52
- Marquette J. B., Rebrion C., Rowe B. R., 1988, *J. Chem. Phys.*, 89, 2041
- Marston G., Nesbitt F. L., Nava D. F., Payne W. A., Stief L. J., 1989, *J. Phys. Chem.*, 93, 5769
- Marty B., Zimmermann L., Burnard P. G., Wieler R., Heber V. S., Burnett D. L., Wiens R. C., Bochsler P., 2010, *Geochim. Cosmochim. Acta*, 74, 340
- Mendes M. B. et al., 2012, *ApJ*, 746, L8
- Milam S. N., Savage C., Brewster M. A., Ziurys L. M., Wyckoff S., 2005, *ApJ*, 634, 1126
- Minissale M., Dulieu F., Cazaux S., Hocuk S., 2016, *A&A*, 585, A24
- Ohishi M., McGonagle D., Irvine W. M., Yamamoto S., Saito S., 1994, *ApJ*, 427, L51
- Pratap P., Dickens J. E., Snell R. L., Miralles M. P., Bergin E. A., Irvine W. M., Schloerb F. P., 1997, *ApJ*, 486, 862
- Redaelli E., Bizzocchi L., Caselli P., Harju J., Chacon-Tanarro A., Leonardo E., Dore L., 2018, *A&A*, in press
- Ritchey A. M., Federman S. R., Lambert D. L., 2011, *ApJ*, 728, 36
- Roberts H., Herbst E., Millar T. J., 2003, *ApJ*, 591, L41
- Rodgers S. D., Charnley S. B., 2008a, *ApJ*, 689, 1448
- Rodgers S. D., Charnley S. B., 2008b, *MNRAS*, 385, L48
- Romano D., Matteucci F., Zhang Z. Y., Papadopoulos P. P., Ivison R. J., 2017, *MNRAS*, 470, 401
- Roueff E., Loison J. C., Hickson K. M., 2015, *A&A*, 576, A99
- Ruad M., Loison J. C., Hickson K. M., Gratier P., Hersant F., Wakelam V., 2015, *MNRAS*, 447, 4004
- Ruad M., Wakelam V., Hersant F., 2016, *MNRAS*, 459, 3756
- Semaniak J. et al., 2001, *ApJS*, 135, 275
- Slinger T. G., Black G., 1982, *J. Chem. Phys.*, 77, 2432
- Taniguchi K., Saito M., 2017, *PASJ*, 69, L7
- Terzieva R., Herbst E., 2000, *MNRAS*, 317, 563
- Turner B. E., Terzieva R., Eric H., 1999, *ApJ*, 518, 699
- Vidal T. H. G., Loison J. C., Jaziri A. Y., Ruad M., Gratier P., Wakelam V., 2017, *MNRAS*, 469, 435
- Wakelam V. et al., 2015, *ApJS*, 217, 20
- Wakelam V., Loison J. C., Mereau R., Ruad M., 2017, *Mol. Astrophys.*, 6, 22
- Wirström E. S., Charnley S. B., Cordiner M. A., Milam S. N., 2012, *ApJ*, 757, L11
- Wirström E. S., Charnley S. B., 2018, *MNRAS*, 474, 3720

APPENDIX: THEORETICAL CALCULATIONS ON THE $\text{H} + {}^{15}\text{NNH}^+ \rightarrow \text{H} + \text{N}^{15}\text{NH}^+$ REACTION

Relative energies at the M06-2X/VTZ (in kJ mol^{-1} at 0 K including ZPE) with respect to the $\text{H} + \text{N}_2\text{H}^+$ energy, geometries, and frequencies (in cm^{-1} , unscaled) of the various stationary points. The absolute energies at the M06-2X/VTZ level including ZPE in hartree are also given in column 1.

Species (energy, hartree)	Relative energies (kJ mol^{-1})	Geometries (Angstrom)				Harmonic frequencies (cm^{-1})
H (−0.4981348)						
${}^{15}\text{NNH}^+$ (−109.708017)	0	N	0.0	0.0	0.646077	755, 755, 2406, 3395
		N	0.0	0.0	−0.435410	
		N	0.0	0.0	−1.474664	
TS (−110.201440)	+12.4	N	−0.106902	−0.555629	0.0	459, 545, 760, 2264,
		N	−0.106902	0.539452	0.0	3390, 814i (imaginary
		H	0.018049	1.565755	0.0	frequency)
		H	1.478578	−1.452517	0.0	

This paper has been typeset from a $\text{T}_\text{E}\text{X}/\text{L}_\text{A}\text{T}_\text{E}\text{X}$ file prepared by the author.